Implementation of Basic Reflex Functions on Musculoskeletal Robots Driven by Pneumatic Artificial Muscles

Ryu Takahashi, Yanlin Wang, Junqi Wang, Yelin Jiang, and Koh Hosoda, *Senior Member, IEEE*

***Abstract*—Musculoskeletal robots hold significant potential for the design of future robots. One of the challenges is the possibility of output delays from the muscles, which may prevent higher centers from compensating during sudden disturbances. The reflex system, widely observed in animals, is viewed as an efficient mechanism for overcoming this challenge. Specifically, the Ia and Ib reflex pathways, as the sensory pathways originating from muscle sensory receptors, are considered to contribute to the responsiveness and convergence of the feedback system with the dynamics of the musculoskeletal body. In this study, we propose a basic reflex system that can be implemented into a robot arm driven by pneumatic artificial muscles (PAMs) and investigate its effectiveness through two experiments: a sudden force shock and a position constraint. The results demonstrate that the reflex behavior is capable of reducing the impact of disturbances, with the Ia reflex pathways providing an immediate response to disturbances and the Ib reflex pathways curbing excessive output force.**

***Index Terms*—Biomimetics, humanoid robot systems, soft robot applications.**

I. Introduction

MUSCULOSKELETAL robots inspired by human musculoskeletal structures have been studied and developed for many years [1], [2], [3], [4]. Their flexible and redundant structure offers a desirable degree of adaptability to unstructured environments, a feature that is absent in traditional motor-driven robots. Pneumatic Artificial Muscles (PAMs) are the most widely employed actuators for these types of robots, due to several advantages including the high power-to-weight ratio, inherent compliance, and close similarities with the kinematics of natural skeletal muscles [5], [6], [7], [8], [9].

On the other hand, like human muscles, PAMs have a large output delay relative to electric motors. If a sudden disturbance impacts the PAM-driven robot and the motion trajectory is corrected by a high-level controller such as the brain, the impact of the disterbance may persist over time and result in damage to the system. Previous research has primarily centered around streamlining the control architecture through the incorporation of well-designed musculoskeletal bodies and the utilization of feedforward controllers [10], [11], [12], [13]. Among the studies that have addressed the controllers for PAMs, proposals have been made for adaptive control [14], [15], [16], [17], energy-based control [18], and bio-inspired neuromuscular control [19], [20], [21], however, none of these methods have yet proven effective in producing an immediate response to reduce the impact of disturbances.

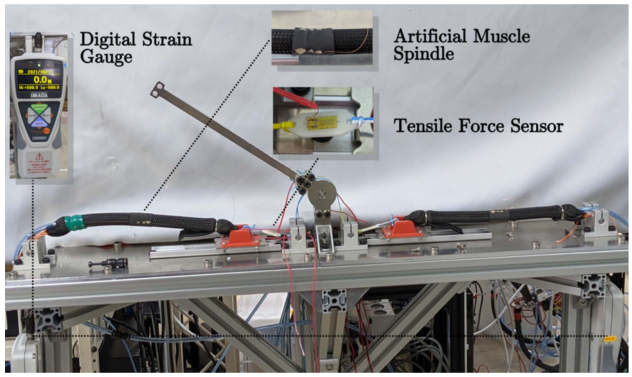

Fig. 1. Experimental setup of the musculoskeletal robot arm.

It is widely recognized within the human and animal neural systems that sensory information obtained from muscle spindles and Golgi tendon organs (GTOs) plays a crucial role in generating spinal reflexes that counteract disturbances [22]. The Ia sensory pathways originating from muscle spindles are related to stretch reflexes, and are capable of immediately responding to sudden change in muscle length. Meanwhile, the Ib sensory pathways originating from GTOs are related to autogenic inhibition reflexes, and they possess the ability to inhibit muscle activity in response to excessive muscle tension [23], [24], [25]. The integration of these sensory pathways into a PAM-driven robot is expected to enable the robot to be adaptable to diverse disturbances.

The objective of this study is to incorporate two distinct types of reflex pathways in a musculoskeletal robot, to detect muscle sensory information and thus reduce the negative impact of

Manuscript received 13 September 2022; accepted 27 January 2023. Date of publication 15 February 2023; date of current version 21 February 2023. This letter was recommended for publication by Associate Editor Y. Peng and Editor X. Liu upon evaluation of the reviewers' comments. This work was supported in part by Osaka University Humanware Innovation Program (HWIP). *(Corresponding author: Ryu Takahashi.)*

The authors are with the Graduate School of Engineering Science, Osaka University, Osaka 565-0871, Japan (e-mail: takahashi.ryu@arl.sys.es.osaka-u.ac.jp; wang.yanlin@arl.sys.es.osaka-u.ac.jp; wang.junqi@arl.sys.es.osaka-u.ac.jp; jiang.yelin@arl.sys.es.osaka-u.ac.jp; hosoda@sys.es.osaka-u.ac.jp).

This letter has supplementary downloadable material available at https://doi.org/10.1109/LRA.2023.3245403, provided by the authors.

Digital Object Identifier 10.1109/LRA.2023.3245403

disturbances. We developed a musculoskeletal robot arm powered by PAMs and equipped with biologically-inspired sensors (corresponding to muscle spindles and GTOs [26], [27]). The system was structured to imitate Ia and Ib sensory pathways and translate the output of these sensors into activation patterns of the PAMs. We experimentally evaluated the functional efficacy of these reflex pathways under the two scenarios: 1) the application of unexpected force shocks to the robot arm and 2) the encounter of an immovable obstacle in the robot's trajectory.

II. Robot Design

A. Biological Foundation

In the neural reflex system, there are two pathways: the Ia pathway, which is innervated by muscle spindles, and the Ib pathway, which is innervated by Golgi tendon organs (GTOs). In this work, we refer to the former as the Ia reflex pathway and the latter as the Ib reflex pathway. In the Ia reflex pathway (Fig. 2(a)) when the muscle spindles are stimulated, the Ia afferent nerve fibers from this muscle innervate directly the α motor neurons of the same muscle, leading to its contraction [28]. This mechanism constitutes a stretch reflex, preventing the muscle from excessive lengthening. The Ia fibers not only excite the motor neurons innervating the same (homonymous) muscle, but also those innervating other (heteronymous) muscles with similar mechanical actions. The Ia fibers also establish inhibitory connections with the α motor neurons innervating antagonistic muscles through the Ia inhibitory interneurons. This disynaptic inhibitory pathway is the basis for reciprocal innervation, where the stretching of a muscle results in the relaxation of its antagonists [29]. Muscle spindles are typically stimulated when the muscle is stretched rapidly. The sensory receptor for the Ib reflex pathway is the Golgi Tendon Organ (GTO), which detects muscle tension information (Fig. 2(b)). Upon stimulation of the GTO, the afferent Ib neuron is activated, establishing synapses with both inhibitory and excitatory interneurons within the spinal cord [30]. The inhibitory interneuron mediates autogenic inhibition of the stimulated muscle, while the excitatory interneuron elicits reciprocal excitation of the antagonist muscle. y movements during which the muscles may contract together to overcome external force depending on tasks [29].

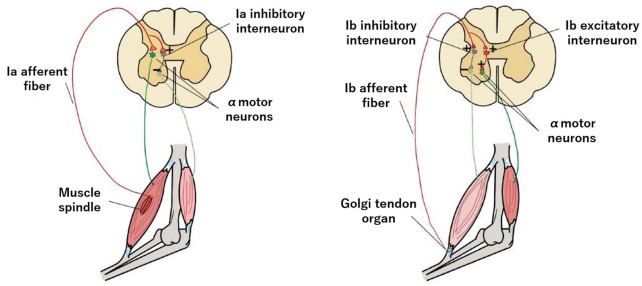

(a) Biological Ia reflex pathway **(b)** Biological Ib reflex pathway

Fig. 2. Biological reflex pathways [29].

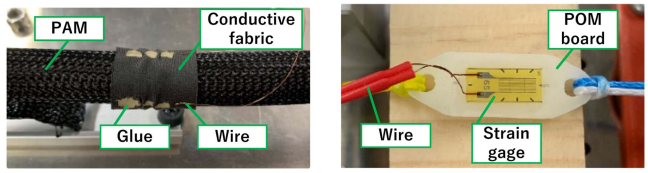

(a) Muscle spindle sensor **(b)** Golgi tendon organ sensor

Fig. 3. Bio-inspired sensors.

B. Bio-Inspired Sensors

In the following sections, we will describe the artificial muscle spindle and GTO sensors, which are the essential components to realize the reflex behaviors in the experiments.

1) Muscle Spindle Sensors: Our previous researches have developed a cost-effective external inflation sensor that does not change the actuator's shape or flexibility [26], [27]. The sensor was made with a conductive stretchable fabric (LTT-SLPA-20 K, EeonTex) that changes the resistance upon stretching. This kind of material has a resistance around several thousand Ω over a 1 cm span. It is designed to be warped around the PAMs (Fig. 3(a)). The fabric sensor lengths change with the circumference of the PAMs, contracting with muscle deflation and stretching with muscle inflation. The high elasticity of the fabric allows sensors to be able to stretch and contract almost synchronously without damaging the muscles. Through the evaluation experiments in our previous research [27], we have concluded that the feedback provided by our fabric sensor is sufficient to indicate the degree of PAM's inflation and detect sudden disturbances.

2) Golgi Tendon Organ Sensors: When the PAM is inflated, it generates radial expansion along with the axial contraction and thereby exerts a pulling force on the load. The force and motion thus generated by this type of actuator are linear and unidirectional. For measuring it, a tension sensor on the axial direction of PAM is required. The position is between the PAM and the link actuated by it. In this system, we used foil strain gauges (KFP-5-120-C1-65L1M2R, Kyowa Electronic Instruments Co., Ltd) to convert the applied tension into an electrical signal. This thin film strain gauge was attached to the surface of a 3 mm polyoxymethylene (POM) board. Then we used fishing line to connect it to the PAM.

C. Mechanical Setup and Hardware Construction

We designed and built a one-joint-arm setup for testing the performance of control strategy, which is essentially an inverted pendulum actuated by a pair of antagonistic PAMs (Fig. 1). Both PAMs had one side fixed on the baseboard and the other side fixed on the linear sliders, which served to constrain the movement of PAMs straightly in the desired direction. The two muscle spindle sensors were wrapped in the middle of our two antagonistic PAMs respectively. Every PAM was connected with a tension sensor via fishing line, then connected to the inverted arm. Because these sensors were hand-crafted, there were large individual differences in sensor values. They have the common

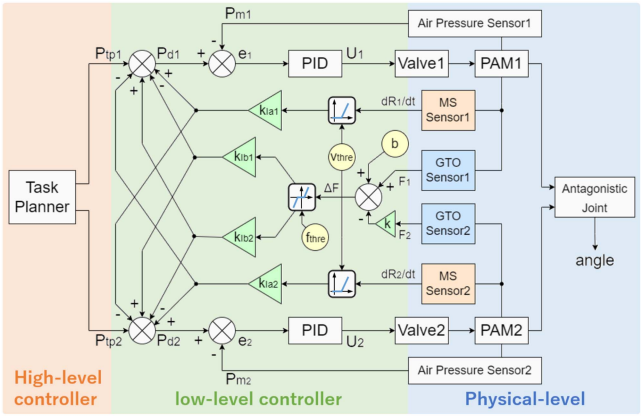

Fig. 4. Schematic diagram of the control system.

output features, which can be addressed by adjusting the gain parameters. We automated the calibration process using the specialized equipments such as the externally mounted digital strain gauge. Besides, an angle encoder is attached on the joint for measuring the angular displacement.

III. Design of Sensory Feedback System

The proposed control system (Fig. 4) is based on the neural reflex method with a hierarchical structure [31]. A pattern generator is implemented as the high-level controller, and three types of movements are designed for this robot system: static states, reaching motion, and rhythmic oscillation, which can be selected prior to the program execution. The reflex system is configured as the low-level controller, and the physical system, including the sensors and the PAMs, is configured at the lowest level. The response of the low-level controller depends on the type and intensity of the stimulus received, resulting in the appearance or suppression of reflex units as appropriate. While hardware limitations prevent the system from being an exact replica of the human reflex system, our aim is to qualitatively imitate the neural reflex mechanism and generating the effective reflex behaviors for the PAM-driven robot system. The sensors operate with a sample rate of 100 Hz. The command frequency of the system is much faster than 100 Hz, which is dependent on the operating system of the microcontroller.

The sensory signal from the embedded muscle spindle sensor is shown by the internal differentiator outputs dR/dt, which indicates how fast the PAM is stretched. This signal is sent to an event trigger based on the deadband in the low-level controller. The Ia reflex pathway is activated when the stretch speed dR/dt of one muscle exceeds the preset threshold v_{thre}, and the corresponding PAM contracts and the antagonistic PAM is relaxed. v_{thre} is set to 10 kΩ/s in the current configuration. The relaxation of the antagonistic PAM leads to an increase in R and dR/dt, which should not be interpreted as a stretch stimulus since it is not caused by any external stimulus. Hence, the low-level controller blocks the activity of reflex units directed towards the antagonistic PAM for the duration of the response, thereby guaranteeing the mutual exclusivity of each reflex pathway process and avoiding unintended oscillations.

The sensory signals from the GTO sensors are converged by the low-level controller and then calibrated using two constants k and b to eliminate the difference in linear expansion coefficient and initial resistance between the two tension sensors with the following equation:

$$\Delta F = F_1 - k \cdot F_2 + b \tag{1}$$

The subscripts 1 and 2 in the variables indicate the left and right antagonistic PAMs, respectively. Each tension value is expressed as F_1 and F_2, and ΔF represents the relative tension. The current system is operating with k at 0.56 and b at 6200. ΔF equals to zero in equilibrium. ΔF is the difference between the two muscle tension and can take either the positive or the negative value. Once $|\Delta F|$ is greater than the preset threshold f_{thre}, which is the calibrated value of the output voltage of the tension sensor, the low-level controller would activate the reflexes on the Ib reflex pathway for the PAM, performing as relaxation of PAM that is bearing higher tension and excitation of opposite PAM for coordination. f_{thre} are set to 1 V. The sensory information from the low-level controller and the descending commands from the high-level controller converge to the output of the final motor command. This process is similar to that of α motor neurons in the human spinal cord. In a robotic system, the motor command is determined according to the following equation:

$$P_{\text{d1}} = P_{\text{tp1}} + \Delta P_{\text{Ia,exci1}} - \Delta P_{\text{Ia,inhi2}} - \Delta P_{\text{Ib,inhi1}} + \Delta P_{\text{Ib,exci2}} \tag{2}$$

$$P_{\text{d2}} = P_{\text{tp2}} + \Delta P_{\text{Ia,exci2}} - \Delta P_{\text{Ia,inhi1}} - \Delta P_{\text{Ib,inhi2}} + \Delta P_{\text{Ib,exci1}} \tag{3}$$

P_{d} are the target air pressure of the PAMs. P_{tp1} and P_{tp2} are the descending motor commands from the task planner. They are sent to the PID controllers, which adjust the proportional valves so that the air pressure of the PAMs are tracking them. $\Delta P_{\text{Ia,exci}}$, $\Delta P_{\text{Ia,inhi}}$, $\Delta P_{\text{Ib,inhi}}$ and $\Delta P_{\text{Ib,exci}}$ are the stretch reflex excitation, the reciprocal inhibition on the Ia pathway and the autogenic inhibition, the reciprocal excitation on the Ib pathway, respectively. The reflex units have a total of 8 parameters for the excitation and inhibition of the Ia and Ib in the two muscles. For the simplicity, we used the same values for 1 and 2, excitation and inhibition, and summarized them into 2 constants. In other words, $k_{\text{Ia,exci1}}$, $k_{\text{Ia,inhi1}}$, $k_{\text{Ia,exci2}}$, $k_{\text{Ia,inhi2}}$ are summarized into k_{Ia}, and $k_{\text{Ib,exci1}}$, $k_{\text{Ib,inhi1}}$, $k_{\text{Ib,exci2}}$, $k_{\text{Ib,inhi2}}$ are summarized into k_{Ib}. In Fig. 4, the reflex units to distinguish the excitation and inhibition are excluded. The response of these reflex units are calculated by the following equations:

$$\Delta P_{\text{Ia}} = k_{\text{Ia}} \cdot dR/dt \tag{4}$$

$$\Delta P_{\text{Ib}} = k_{\text{Ib}} \cdot (\Delta F - f_{\text{thre}}) \tag{5}$$

The parameters used in this control system are listed in Table I. These parameters were empirically determined.

TABLE I
PARAMETERS OF THE REFLEX UNITS

Parameter	Definition	Value (units)
k_{Ia}	Constant for Ia reflex pathway	1/80000
k_{Ib}	Constant for Ib reflex pathway	1/300
v_{thre}	Threshold for stretch speed	10 (kΩ/s)
f_{thre}	Threshold for muscle tension	1 (V)
k	Constant for calculating ΔF	0.56
b	Constant for calculating ΔF	6200

IV. RESULTS

The two reflex pathways described above share the goal of protecting the body, but their characteristics are contrasting: the Ia reflex pathway works for the immediate excitation and the Ib reflex pathway works for the gradual inhibition. It is not clear how these reflex pathways coexist in the human neral system. Here, we experimentally demonstrated the function of each reflex pathway by exploring scenarios in which each pathway works effectively. We thus designed three experiments under different conditions. Firstly, we confirmed that the robot was capable of producing the basic movements without disturbances. Secondly, the robot was applied to unexpected force shocks. We verified that the responsiveness of the stretch reflex, elicited by the Ia reflex pathways, to the disturbance. Finally, the robot arm encountered an immovable obstacle before reaching the target position. We verified the efficacy of the autogenic inhibition elicited by the Ib reflex pathways could prevent the robot from continuing to apply force against the obstacle. It is important to note that each reflex pathway was individually evaluated.

A. Free Movements

We set the task planner to sending sinusoidal commands to the PAMs. The cycle rate was set to 3 s. The robot system is supposed to oscillate on a sinusoidal basis by actuating the PAMs without any disturbance. Sensor signals were continuously sampled in the process to check whether they correctly reflected the system status. The following experiments are conducted with a sampling rate of 100 Hz. The joint angle is positive at the left side and negative at the right side. The commands of the two PAMs had a phase shift of π to generate oscillation movement. Fig. 5 shows that the all signals change with the oscillation of the joint angle. The system was able to move the robot arm smoothly and the sensor responses to the movements were as expected.

B. Immediate Response Against Disturbances

A pendulum with load 1 kg was placed over the robot system. The pendulum length was 30 cm and the falling angle was set around 45° for ease of the observation. When the load was released, it impacted the robot arm, inducing a displacement in the joint angle. The force shocks were applied five times in a row in one experiment without interference between them. The Ia reflex pathway of the stretched PAM was stimulated and the PAM contracted. As shown in Fig. 6(b), the desired reflex

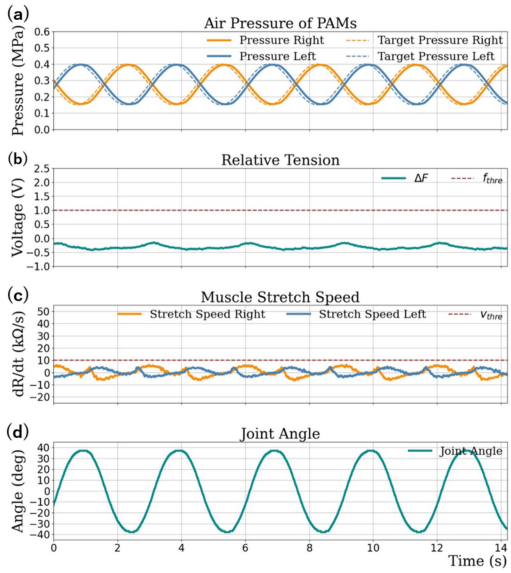

Fig. 5. Sensor signals during the oscillation movement in the cycles of 3 s. (a) Measured (solid lines) and target (dashed lines) air pressures in the PAMs. (b) Calculated voltage from the tension sensors, which represents the relative tension ΔF, and the threshold f_{thre}. (c) dR/dt that represents the similar trend of the stretch speed of the PAM, and the threshold v_{thre}. (d) Joint angle of the robot arm. The dR/dt values were the low-pass filtered values (the cutoff frequency was 10 Hz).

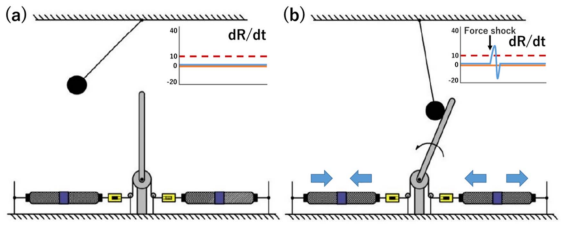

Fig. 6. (a) Experimental setup for force shocks. (b) The expected response in the robot system.

response was to counteract the force shock and to reduce the negative effect of the force shock as quickly as possible.

We hypothesized that the reflex response could decrease the angular displacement caused by the force shock. Two groups of experiments, with and without the Ia reflex pathways, were conducted. Fig. 7(a) plotted the sensor signals with the Ia reflex pathways. All the signals remain in the steady state before the collision. When the collision occurs, the stretch speed dR/dt of the left PAM immediately increases and exceeds the threshold v_{thre}. As a result, the target air pressure of the left PAM increases, the target air pressure of the right PAM decreases, and the reflex behavior is generated. The low level controller takes around 40 ms to detect the stimuli. To make the PAMs work effectively against the disturbance, the system keeps the reflex command for 200 ms, considering the output delay of the PAM. The reflex behavior passively stretched the right PAM and its dR/dt also increased rapidly. The increase is larger than the left-hand side, but is ignored by the system as described above. The Joint angle was rotated to the negative direction by the force shock and then rotated to the opposite directions

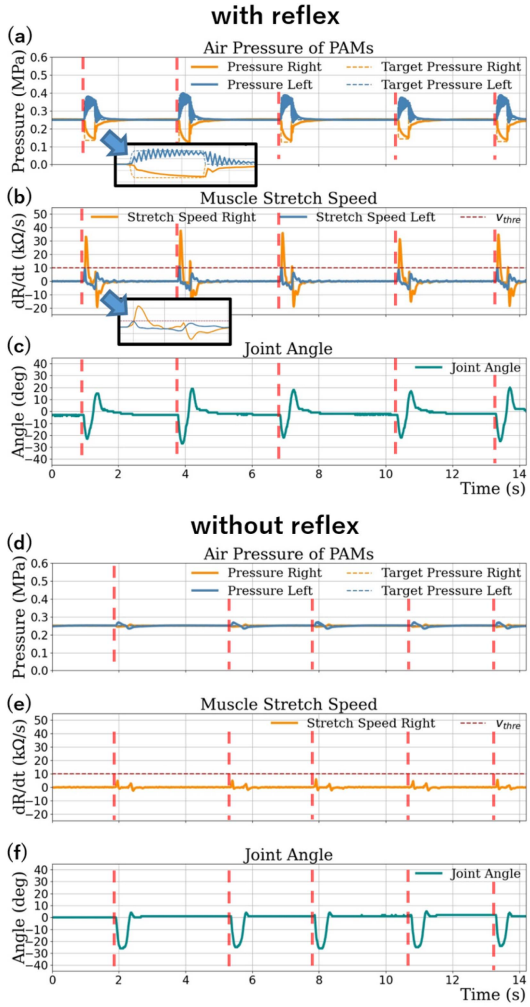

Fig. 7. (a)–(c) Reflex responses to the force shocks with the Ia reflex pathway and (d)–(f) original response to them without the reflex. The red dashed lines show the timing of the force shocks. (a) and (d) The measured (solid lines) and the target (dashed lines) air pressures in the PAMs. (b) and (e) The dR/dt values that represents the similar trend of the stretch speed of the PAM, and the threshold v_{thre}, and (c) and (f) the joint angle of the robot arm.

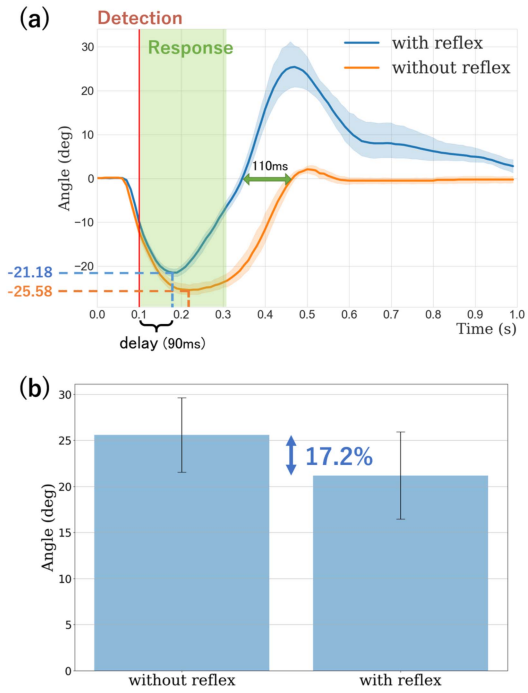

Fig. 8. (a) Detailed angular displacements are shown as the mean of the 20 trials with the 95% confidence intervals. The blue line is the joint angle with the Ia refrex pathways and the orange line is without it. The vertical red line indicates the timing when the controller detects the stimulus. the average angular displacements were 21.18 and 25.58, respectively. The delayed-time to come back the joint angle to 0° was reduced 110 ms by the reflex behavior. (b) Comparison of the angular displacements with and without the reflex are shown as the mean with the ± 2 SD error bar. The angular displacement with the reflex decreased 17.2% than that without it.

by the reflex response. Finally, the joint return to the middle position. The results in Fig. 7(b) show what the original response would be without the Ia reflex pathways. It can be seen that there is a slight pressure fluctuation in the left PAM due to the shock. The PID controller is controlled to maintain the air pressure in both PAMs at 0.25 MPa. As for the angular information, it shows a uniform angular displacement for each shock.

We compared the joint angles in two cases with and without the Ia reflex pathways to investigate how they affect the robot behavior. Fig. 8(a) shows the detailed plots of how the robot responds to a force shock over one second periods. It can be seen that the robot with the Ia reflex pathways could reduce the angular displacement compared to that of the robot without it. Fig. 8(b) compares the angular displacements of both robots, which are 25.58 and 21.18, respectively. This means the reflex reduced the angular displacement by 17.2%. On the other hand, following the reflex behavior, there was a large recoil in the positive direction. The reason is that the gain K_{Ia} was set large enough to allow for the reflex behavior to be sufficiently responsive. It occurs in humans as well, for example, when the patellar tendon reflex that is triggered by a sharp tap just below the knee is overactive in response to stretching the patellar tendon. From the perspective of classical control theory, it is natural to assume that the system becomes oscillatory when the responsiveness increases, and an additional factor is required to reduce this recoil. The Ib reflex pathways, discussed in the next experiment, have the ability to inhibit the output of the muscle and could be the candidate for the factor. In human neural system, the Ia and Ib reflex pathways may compensate for each other's characteristics, such as P-gain and D-gain in PID control. The results also show a considerable latency around 90 ms until the joint starts moving back from detecting stimuli. The response of this system is relatively slower than the human reflex response (around 50 ms [32]). This is caused by the larger output delay of PAMs than that of human muscles.

C. *Autogenous Inhibition Against Positional Constraints*

A robot operating in a reak environment has the opportunity to face ummobile obstacles on their motion trajectory. If the robot continues to drive the actuator against the position constraint (Fig. 9(a)), the contact force will increase and the robot might be broken. It is expected that the autogenic inhibition by the Ib

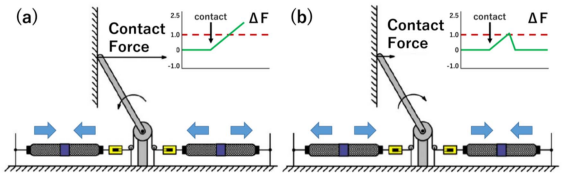

Fig. 9. (a) Experimental setup for a position constraint. (b) The expected response in the robot system.

reflex pathway could work to stop the robot without forcing it to continue the motion.

In this experiment, the task planner was designed to be moving from the right side to the left side, and the obstacle is placeed between left side and middle position of robot arm. The low-level controller was monitoring whether the relative tension $|\Delta F|$ exceeded the threshold, and the excessive tension $\Delta F - f_{\text{thre}}$ was innervated through the Ib reflex pathway according to the polarity. The reflex behaviors should contain the contraction of the primary actuating PAM and the expansion of the other PAM as shown in Fig. 9(b), resulting in a decrease or disappearance of the contact force. The reflex response lasted for 200 ms, which was the same as the duration of the Ia reflex response. In this research, the post reflex status was designed to be keeping the static state.

Fig. 10(a) shows the related sensor signals during the working process. The robot starts contacting with the obstacle at around 2.1 s, which is marked by a vertical red line. Then, we could observe that the relative tension ΔF starts increasing. At around 2.9 s marked by a vertical green line, ΔF reaches the threshold. Then, the left PAM starts deflating and the other PAM starts inflating, and the relative tension decreases to around zero. In the system without the Ib reflex pathways, the relative tension continues to increase after the contact with the position constraint (Fig. 10(b)). This response prevents the robot from continuous driving, releases the contact force between the robot and obstacles. The results showed that the Ib reflex pathway worked on inhibiting the internal muscle output and could contribute to protecting the robot itself.

V. Conclusion

This study proposed a basic reflex system implemented into a robot arm driven by pneumatic artificial muscles (PAMs). The control architecture is based on the human neural system, which consists of a high-level controller to generate the motion patterns and a low-level controller to generate the reflex behaviors against disturbances. Through the three experiments, we verified the basic operation of the task planner without disturbances, the responsiveness of the Ia reflex pathways to force shocks, and the autogenic inhibition of the Ib reflex pathways to a position constraint. When the robot was subjected to a force shock, the reflex behavior effectively reduced the angular displacement. This effect has not been achieved with the previous PAM-driven robots. For a positional constraint, the robot detected the contact with an obstacle by the Ib reflex pathways and showed a response to inhibit the motion.

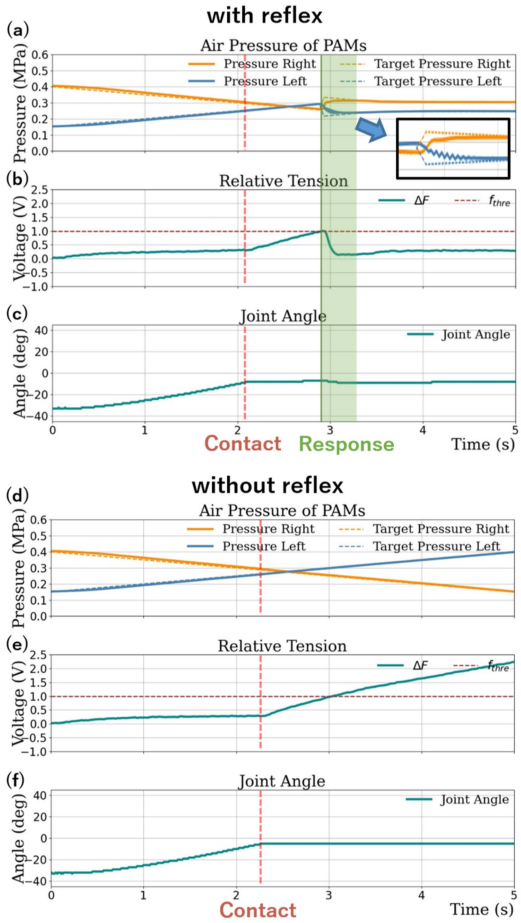

Fig. 10. (a)–(c) Reflex responses to a position constraint with the Ib reflex pathway and (d)–(f) original response to it without the reflex. The red dashed line shows the timing of the contact. (a) and (d) The measured (solid lines) and the target (dashed lines) air pressures in the PAMs. (b) and (e) The ΔF values that represents the related tension of the PAMs, and the threshold f_{thre}, and (c) and (f) the joint angle of the robot arm.

It might seem that excitatory Ia and inhibitory Ib reflex pathways have opposing features, and it was not clear in neuroscience how they coexist. In this letter, we demonstrated the feature of each reflex pathway by considering individual scenarios in which each pathway is effective. This allowed us to investigate the qualitative properties of each reflex pathway, even when the control parameters used in the experiments were different from those in the living system. The question of how to add (or subtract, or time-delayed responses) will become an issue in more complex scenarios where both pathways work, but this is envisioned as a future research roadmap. In this scenario, we plan to devise a way to use control parameters that are similar to the living system. We take into account the measurement of contact forces produced at the point of impact, to demonstrate clearly that the reflex behavior can avoid the damage on the robot and the surrounding environment. Additionally, it is easy to imagine expanding the low-level controller of this system by assembling a network of reflex pathways and applying it to arms and legs with more complex structures. This is expected to improve the adaptability of the musculoskeletal robot in its various motions.

ACKNOWLEDGMENT

The authors would like to thank Yiqi Li for his help to conduct our experiments and the valuable suggestions to improve the quality of this letter.

REFERENCES

[1] B. Verrelst, R. Van Ham, B. Vanderborght, F. Daerden, D. Lefeber, and J. Vermeulen, "The pneumatic biped "Lucy" actuated with pleated pneumatic artificial muscles," *Auton. Robots*, vol. 18, no. 2, pp. 201–213, 2005.

[2] K. Hosoda, T. Takuma, A. Nakamoto, and S. Hayashi, "Biped robot design powered by antagonistic pneumatic actuators for multi-modal locomotion," *Robot. Auton. Syst.*, vol. 56, no. 1, pp. 46–53, 2008.

[3] R. Niiyama and Y. Kuniyoshi, "Design of a musculoskeletal Athlete robot: A biomechanical approach," in *Mobile Robotics: Solutions and Challenges*. Singapore: World Scientific, 2010, pp. 173–180.

[4] S. Ikemoto, Y. Nishigori, and K. Hosoda, "Advantages of flexible musculoskeletal robot structure in sensory acquisition," *Artif. Life Robot.*, vol. 17, no. 1, pp. 63–69, 2012.

[5] H. Schulte, "The characteristic of the McKibben artificial muscle," in *The Application of External Power in Prosthetics and Orthetics*. Washington, DC, USA: National Academy of Sciences, Appendix H, Publication 874, pp. 94–115.

[6] C.-P. Chou and B. Hannaford, "Measurement and modeling of McKibben pneumatic artificial muscles," *IEEE Trans. Robot. Automat.*, vol. 12, no. 1, pp. 90–102, Feb. 1996.

[7] B. Tondu and P. Lopez, "The McKibben muscle and its use in actuating robot-arms showing similarities with human arm behaviour," *Ind. Robot: Int. J.*, vol. 24, no. 6, pp. 432–439, 1997.

[8] B. Tondu and P. Lopez, "Modeling and control of McKibben artificial muscle robot actuators," *IEEE Control Syst. Mag.*, vol. 20, no. 2, pp. 15–38, Apr. 2000.

[9] B. Tondu, "Modelling of the McKibben artificial muscle: A review," *J. Intell. Mater. Syst. Struct.*, vol. 23, no. 3, pp. 225–253, 2012.

[10] Y. K. Lee and I. Shimoyama, "A Skeletal Framework Artificial Hand Actuated by Pneumatic Artificial Muscles," in *Morpho-Functional Machines: The New Species*. Springer, 2003, pp. 131–143.

[11] B. Tondu, S. Ippolito, J. Guiochet, and A. Daidie, "A seven-degrees-of-freedom robot-arm driven by pneumatic artificial muscles for humanoid robots," *Int. J. Robot. Res.*, vol. 24, no. 4, pp. 257–274, 2005.

[12] Y. Okadome, Y. Nakamura, K. Urai, Y. Nakata, and H. Ishiguro, "HUMA: A human-like musculoskeletal robot platform for physical interaction studies," in *Proc. IEEE-RAS 15th Int. Conf. Humanoid Robots*, 2015, pp. 676–683.

[13] A. Hitzmann, H. Masuda, S. Ikemoto, and K. Hosoda, "Anthropomorphic musculoskeletal 10 degrees-of-freedom robot arm driven by pneumatic artificial muscles," *Adv. Robot.*, vol. 32, no. 15, pp. 865–878, 2018.

[14] A. Bicchi, G. Tonietti, and E. Piaggio, "Design, realization and control of soft robot arms for intrinsically safe interaction with humans," in *Proc. IARP/RAS Workshop Tech. Challenges Dependable Robots Hum. Environ.*, 2002, pp. 79–87.

[15] G. Tonietti and A. Bicchi, "Adaptive simultaneous position and stiffness control for a soft robot arm," in *Proc. IEEE/RSJ Int. Conf. Intell. Robots Syst.*, 2002, vol. 2, pp. 1992–1997.

[16] T. Karnjanaparichat and R. Pongvuthithum, "Adaptive control for a one-link robot arm actuated by pneumatic muscles," *Chiang Mai J. Sci*, vol. 35, no. 3, pp. 437–446, 2008.

[17] H. P. H. Anh, N. N. Son, and C. Van Kien, "Adaptive neural compliant force-position control of serial PAM robot," *J. Intell. Robot. Syst.*, vol. 89, no. 3, pp. 351–369, 2018.

[18] D. Liang, N. Sun, Y. Wu, Y. Chen, Y. Fang, and L. Liu, "Energy-based motion control for pneumatic artificial muscle actuated robots with experiments," *IEEE Trans. Ind. Electron.*, vol. 69, no. 7, pp. 7295–7306, Jul. 2022.

[19] B. Hannaford, J. M. Winters, C.-P. Chou, and P.-H. Marbot, "The anthroform biorobotic arm: A system for the study of spinal circuits," *Ann. Biomed. Eng.*, vol. 23, no. 4, pp. 399–408, 1995.

[20] C.-H. Wu, K.-S. Hwang, and S.-L. Chang, "Analysis and implementation of a neuromuscular-like control for robotic compliance," *IEEE Trans. Control Syst. Technol.*, vol. 5, no. 6, pp. 586–597, Nov. 1997.

[21] S. Eskiizmirliler, N. B. Forestier Tondu, and C. Darlot, "A model of the cerebellar pathways applied to the control of a single-joint robot arm actuated by McKibben artificial muscles," *Biol. Cybern.*, vol. 86, no. 5, pp. 379–394, 2002.

[22] E. Liddell and C. Sherrington, "Reflexes in response to stretch (myotatic reflexes)," *Proc. Roy. Soc. London. Ser. B., Containing Papers Biol. Character*, vol. 96, no. 675, pp. 212–242, 1924.

[23] M. C. Brown and P. Matthews, "On the subdivision of the efferent fibres to muscle spindles into static and dynamic fusimotor fibres," in *Control and Innervation of Skeletal Muscle*. London, U.K.: E. S. Livingstone, 1966, pp. 18–31.

[24] I. Boyd, "The isolated mammalian muscle spindle," *Trends Neurosci*, vol. 3, pp. 258–265, 1980.

[25] J. E. Swett and T. W. Schoultz, "Mechanical transduction in the Golgi tendon organ: A hypothesis," *Arch. Italiennes de Biologie*, vol. 113, no. 4, pp. 374–382, 1975.

[26] A. Hitzmann, S. Ikemoto, and K. Hosoda, "Highly-integrated muscle-spindles for pneumatic artificial muscles made from conductive fabrics," in *Proc. Conf. Biomimetic Biohybrid Syst.*, 2019, pp. 171–182.

[27] A. Hitzmann, Y. Wang, T. Kessler, and K. Hosoda, "Using conductive fabrics as inflation sensors for pneumatic artificial muscles," *Adv. Robot.*, vol. 35, no. 16, pp. 995–1011, 2021.

[28] M. Hulliger, "The mammalian muscle spindle and its central control," in *Reviews of Physiology, Biochemistry and Pharmacology*, vol. 101. Berlin, Germany: Springer, 1984, pp. 1–110.

[29] E. R. Kandel et al., *Principles of Neural Science*, vol. 4. New York, NY, USA: McGraw-Hill, 2000.

[30] J. C. Moore, "The Golgi tendon organ: A review and update," *Amer. J. Occup. Ther.*, vol. 38, no. 4, pp. 227–236, 1984.

[31] G. E. Loeb, I. E. Brown, and E. J. Cheng, "A hierarchical foundation for models of sensorimotor control," *Exp. Brain Res.*, vol. 126, no. 1, pp. 1–18, 1999.

[32] N. Mamizuka, M. Sakane, K. Kaneoka, N. Hori, and N. Ochiai, "Kinematic quantitation of the patellar tendon reflex using a Tri-axial accelerometer," *J. Biomech.*, vol. 40, no. 9, pp. 2107–2111, 2007.